



Platelet-Rich Plasma Greatly Potentiates Insulin-Induced Adipogenic Differentiation of Human Adipose-Derived Stem Cells Through a Serine/Threonine Kinase Akt-Dependent Mechanism and Promotes Clinical Fat Graft Maintenance

VALERIO CERVELLI,^{a*} MARIA G. SCIOLI,^{b*} PIETRO GENTILE,^a ELENA DOLDO,^b ELENA BONANNO,^b LUIGI G. SPAGNOLI,^b AUGUSTO ORLANDI^b

Key Words. Human adipose tissue-derived stem cells • Platelet-rich plasma • Insulin • Adipogenesis • Akt • Fat grafting

ABSTRACT

The potential plasticity and therapeutic utility in tissue regeneration of human adipose-derived stem cells (ASCs) isolated from adult adipose tissue have recently been highlighted. The use of autologous platelet-rich plasma (PRP) represents an alternative strategy in regenerative medicine for the local release of multiple endogenous growth factors. Here we investigated the signaling pathways and effects of PRP and human recombinant insulin on proliferation and adipogenic differentiation of ASCs in vitro. PRP stimulated proliferation ($EC_{50} = 15.3 \pm 1.3\%$ vol/vol), whereas insulin's effect was the opposite ($IC_{50} = 3.0 \pm 0.5 \mu M$). Although PRP alone did not increase adipogenesis, in association with insulin it prevented ASC proliferative arrest, greatly enhanced intracytoplasmic lipid accumulation, strongly increased serine/threonine kinase Akt phosphorylation and mouse monoclonal anti-sterol regulatory element binding protein-1 accumulation, and downregulated Erk-1 activity; adipogenic effects were markedly prevented by the Akt inhibitor wortmannin. PRP with insulin synergistically upregulated fibroblast growth factor receptor (FGFR) and downregulated epidermal growth factor receptor (ErbB) expression; moreover, PRP in association prevented insulin-induced insulin-like growth factor-1 receptor and insulin receptor downregulation. The inhibition of FGFR-1, epidermal growth factor receptor (EGFR), and epidermal growth factor receptor-2 (ErbB2) activity reduced ASC proliferation, but only that of FGFR-1 reduced adipogenesis and Akt phosphorylation, whereas the ErbB2 inhibition effects were the opposite. However, EGFR activity was needed for ErbB2-mediated inhibition of ASC adipogenesis. Clinically, the injection of insulin further ameliorated patients' 1-year PRP-induced fat graft volume maintenance and contour restoring. Our results ascertain that PRP in association with insulin greatly potentiates adipogenesis in human ASCs through a FGFR-1 and ErbB2-regulated Akt mechanism. The ameliorated clinical fat graft maintenance suggests additional useful translational applications of combined PRP-insulin treatment in regenerative medicine. *STEM CELLS TRANSLATIONAL MEDICINE* 2012;1:206–220

INTRODUCTION

The clinical management of tissue imperfections due to traumatic or postsurgical events, or congenital or chronic debilitating conditions, is crucial for structural and functional reconstruction of tissues and organs [1]. This leads to improving scientific knowledge of tissue engineering-based procedures in reconstructive strategies that include autografts, growth factor use, and the respective use of stem cells. Visceral and subcutaneous adipose tissue has been demonstrated to contain progenitor cells able to differentiate in

multiple cell lineages [2, 3]. After centrifugation of collagenase-digested adult adipose tissue, a heterogeneous cell population named stromal-vascular fraction (SVF) is obtained [3, 4]. After SVF plating, the adherent replicative cells are conventionally termed multipotent adipose tissue-derived stem cells (ASCs) [5, 6]. Although adipose tissue is abundant and easily accessible for autologous tissue replacement, the clinical success of fat grafting is limited by a variable but unpredictable low survival rate [7]. The potential plasticity of ASCs offers tremendous new potential in regenerative medicine and surgery,

^aPlastic Surgery Department and ^bInstitute of Anatomic Pathology, Tor Vergata University, Rome, Italy

*Contributed equally as first authors.

Correspondence: Augusto Orlandi, M.D., Institute of Anatomic Pathology, Department of Biopathology and Image Diagnostics, Tor Vergata University of Rome, Via Montpellier, 00133 Rome, Italy. Telephone: 0039.06.20903960; Fax: 0039.0620902209; e-mail: orlandi@uniroma2.it

Received November 8, 2011; accepted for publication January 12, 2012; first published online in *SCTM EXPRESS* March 7, 2012.

©AlphaMed Press
1066-5099/2012/\$20.00/0

<http://dx.doi.org/10.5966/sctm.2011-0052>

including fat tissue grafting procedures [8]. In normal conditions, tissue damage results in platelet activation and secretion of several biologically active proteins, which are responsible for cellular chemotaxis, proliferation, and differentiation and laying down the extracellular matrix that characterizes tissue healing [9]. The use of autologous platelet-rich plasma (PRP) obtained by blood centrifugation is an alternative and easily controllable strategy for the local release of multiple endogenous growth factors for tissue regeneration [10, 11]. PRP use has been safely documented in many fields, including in maxillofacial surgery and in the treatment of problematic soft tissue ulcers [12, 13]. After activation, PRP releases a pool of growth factors, in particular decreasing amounts of basic fibroblast growth factor (b-FGF), insulin-like growth factor-1 (IGF-1), transforming growth factor- β , platelet-derived growth factor-BB, epidermal growth factor, and vascular endothelial growth factor [14]. Despite some initial contrasting opinions on their effects on ASC proliferation and differentiation [15], platelet-derived growth factors play a prominent, if not deciding, role in fat graft survival [16, 17]. PRP greatly stimulated ASC proliferation *in vitro* [17–20], and this effect was obtained without influencing significantly intracytoplasmic lipid accumulation [20]. It has also been documented that insulin sustains the differentiation of adipocyte precursors [21], and slow insulin delivery in the rat abdominal wall is followed by adipose tissue generation [22]. The serine/threonine kinase Akt represents an initial signaling node within all cells of higher eukaryotes [23]. In particular, Akt contributes significantly to the regulation of survival, growth, proliferation, angiogenesis, and metabolism of many cell types [23]. It has been reported that Akt plays a role in murine 3T3-L1 pre-adipocyte adipogenesis [24]. At present, scarce information is available regarding the role of Akt activity in human ASC adipogenesis and the receptor activity involved in Akt signaling. Here we characterized the effects of insulin and PRP on proliferative and adipogenic differentiation properties of human ASCs and documented that in association PRP sustains proliferation and greatly potentiates insulin-induced adipogenic differentiation through the increase of Akt and Akt-regulated genes activity. The beneficial adipogenic effects of combined PRP and insulin treatment were confirmed by the improvement of long-term maintenance of fat graft in patients undergoing surgical correction of soft tissue defects. The modulation and role of the receptor signaling involved in PRP and insulin-induced upstream activation of Akt pathway are also reported and discussed.

MATERIALS AND METHODS

A detailed description of the methods is available in the supplemental online data. All procedures were performed under written patient informed consent and in accordance with the guidelines of the local Committee on Human Research.

Patients, PRP Preparation, and Fat Grafting Procedures

Thirty-nine patients, selected in a randomized and blinded manner, underwent regenerative soft tissue defect surgery for the reconstruction of three-dimensional projection of soft tissues in the Romberg syndrome, hemifacial atrophy, chemical injuries, or burn sequelae. Clinical details are available in supplemental online Table 1. PRP was obtained by the Cascade-Esforax system during intraoperative fat grafting procedures as reported [20]. For *in vitro* assays, PRPs from 10 ran-

domly selected patients were pooled and stored in small aliquots at -80°C . While asepsis was maintained, liposuction aspirates were purified and implanted with variable volumes of PRP per milliliter of fat tissue (% vol/vol). A cohort of patients ($n = 10$) affected by soft tissue defects and scars were also locally injected with 0.5 ml of insulin ($40\ \mu\text{M}$; Sanofi-Aventis Deutschland GmbH, Frankfurt, Germany, <http://www.sanofi-aventis.com>) 7 and 15 days after PRP-enriched fat grafting. Adipose tissue graft volume maintenance, contour restoring, and patient satisfaction were periodically monitored [20].

Adipose Tissue Harvest and Stem Cell Isolation

Residual fat volumes from lipoaspirates of 12 randomly selected patients following fat grafting procedures were placed in a shaking water bath at 37°C , agitated for 60 minutes, and then centrifuged at $600g$ for 10 minutes at room temperature. ASCs were separated from SVF and cultured as reported [20].

Assessment of Adipogenic, Osteogenic, and Neurogenic Differentiation of Human ASCs

The adipogenic and osteogenic potential of ASCs (supplemental online Fig. 1) was checked as reported [20]. Neurogenic differentiation of ASCs was verified with anti-S100 antibody staining (NeoMarkers, Lab Vision, Fremont, CA, <http://www.labvision.com>).

Effects of PRP and Insulin on ASC Proliferation and Adipogenic Differentiation

ASCs at the third passage were treated with PRP (1%–50% vol/vol), with human recombinant insulin (0.1 – $40\ \mu\text{M}$), and in combination. In some instances, after serum starvation ASCs were treated with variable concentrations of selective inhibitors of epidermal growth factor receptor (EGFR; AG1478, Sigma-Aldrich, St. Louis, <http://www.sigmaaldrich.com>) and epidermal growth factor receptor 2 (ErbB2; AG879, Sigma-Aldrich). In addition, fibroblast growth factor receptor-1 (FGFR-1) (Sigma-Aldrich), FGFRs (Sigma-Aldrich), IGF-1R (Sigma-Aldrich), and phosphatidylinositol 3-kinase/Akt (wortmannin, Sigma-Aldrich) inhibition were induced in the presence of 10% fetal bovine serum (FBS), PRP (5% vol/vol), and insulin ($30\ \mu\text{M}$) for 6 days. Specific inhibition of receptor activity was confirmed by blot analysis. Cells were trypsinized and counted using a hemocytometer, and 3-(4,5-dimethylthiazole-2-yl)-2,5-diphenylterazolium bromide assay was carried out according to the kit protocol (Sigma-Aldrich). Absorbance as optical density units was determined at 570 nm by a microplate reader (Sunrise TECAN, LabX, Midland, ON, Canada, <http://www.tecan.com>). To evaluate adipogenic differentiation, semiquantitative analysis of intracytoplasmic lipid droplet accumulation after Oil Red O staining was performed at $\times 400$ magnification using Scion Image software (Scion Corporation, Frederick, MD, <http://www.scioncorp.com>), and expressed as arbitrary units.

Transmission Electron Microscopy

ASCs were postfixed in 1% OsO_4 for 2 hours and dehydrated through an alcohol series and propylene oxide before being embedded in EPON 812. Ultrathin sections were counterstained with uranyl acetate and lead citrate and studied with a Philips 301 transmission electron microscope (Philips Electron Optics, Eindhoven, The Netherlands, <http://www.research.philips.com>).

Table 1. Clinical data of patients ($n = 39$) and fat grafting procedures

No.	Pt	Age	Sex	Comorbidity	Pathology	Old treatment	Treatment	Complication
1	M.M	36	M	No	Post-traumatic scar	Z-Plastic	Lipostructure + 20% vol/vol PRP	No
2	M.P	42	M	Diabetes	Post-traumatic scar	No. 3 Skin Graft	Lipostructure + 30% vol/vol PRP	No
3	L.A	50	F	No	Postsurgical scar	Breast reconstruction	Lipostructure + 20% vol/vol PRP	No
4	M.F	58	M	No	Postsurgical scar	Fibula Flap	Lipostructure + 30% vol/vol PRP	No
5	N.A	45	M	No	Postsurgical scar	Z-Plastic	Lipostructure + 40% vol/vol PRP	No
6	M.F	23	F	No	Post-traumatic scar	No. 1 lipostructure + Z-Plastic	Lipostructure + 40% vol/vol PRP	No
7	C.F	46	M	Hypertension	Facial soft tissue deficit + post-traumatic scar	Reconstructive surgery	Lipostructure + 20% vol/vol PRP	No
8	F.D	27	F	No	Hemifacial atrophy	Lipostructure	Lipostructure + 20% vol/vol PRP	No
9	S.D	37	F	No	Post-traumatic scar	Skin expander + skin graft	Lipostructure + 30% vol/vol PRP	No
10	M.A	37	F	No	Postsurgical scar	Skin expander + skin graft	Lipostructure + 20% vol/vol PRP	No
11	S.M	43	F	Diabetes	Postsurgical scar	Skin graft + lipostructure	Lipostructure + 30% vol/vol PRP	No
12	P.A	29	F	No	Breast postburn scar	Z-Plastic	Lipostructure + 40% vol/vol PRP	No
13	B.D	18	F	No	Breast postburn scar	No. 2 skin grafts	Lipostructure + 30% vol/vol PRP	No
14	T.A	37	M	No	Post-traumatic scar	Z-Plastic + reconstructive surgery	Lipostructure + 40% vol/vol PRP	No
15	A.S	76	M	Dislipidemy	Facial soft-tissue defect	No	Lipostructure + 30% vol/vol PRP	No
16	P.F	44	M	Romberg disease	Hemifacial atrophy right	No. 1 lipostructure	Lipostructure + 20% vol/vol PRP	No
17	B.H	45	F	Diabetes	Hemifacial atrophy left	Poliglactac acid	Lipostructure + 40% vol/vol PRP	No
18	S.F	35	M	Romberg disease	Hemifacial atrophy right	No. 1 lipostructure	Lipostructure + 40% vol/vol PRP	No
19	T.E	48	M	Diabetes	Post-traumatic scar	Wound complex + no. 1 lipostructure	Lipostructure + 20% vol/vol PRP	No
20	M.F	43	F	No	Post-traumatic scar	Wound complex	Lipostructure + 30% vol/vol PRP	No
21	C.E ^a	48	F	No	Post-traumatic scar	Skin graft; recell	Lipostructure + 50% vol/vol PRP	No
22	C.T ^a	51	F	No	Postsurgical scar	Breast augmentation	Lipostructure + 50% vol/vol PRP	No
23	D.A ^a	30	M	HCV+	Postburn scar	Skin expander + skin graft	Lipostructure + 50% vol/vol PRP	No
24	M.Y ^a	37	F	No	Postburn scar	Skin expander + skin graft	Lipostructure + 50% vol/vol PRP	No
25	A.R ^a	49	F	No	Post-traumatic scar	Ophthalmological surgery	Lipostructure + 50% vol/vol PRP	No
26	P.F ^a	44	M	Romberg disease	Hemifacial atrophy right	No	Lipostructure + 50% vol/vol PRP	No
27	B.D ^a	21	F	No	Postburn scar	No	Lipostructure + 50% vol/vol PRP	No
28	P.A ^a	48	F	No	Post-traumatic scar	No	Lipostructure + 50% vol/vol PRP	No
29	D.M ^a	25	F	Romberg disease	Hemifacial atrophy	No	Lipostructure + 50% vol/vol PRP	No
30	Y.F	29	F	No	Facial postburn scar	Skin expander + skin graft	Lipostructure + 40% vol/vol PRP + insulin after 7, 15 days	No
31	B.G	17	F	Congenital foot wrong	Postsurgical scar	Correction of congenital wrong	Lipostructure + 40% vol/vol PRP + insulin after 7, 15 days	No
32	M.S	53	F	Romberg disease	Hemifacial atrophy left	No. 1 poliglactac acid, no. 1 lipostructure	No. 2 lipostructure + 40% vol/vol PRP + insulin after 7, 15 days	No
33	D.M	37	M	No	Nose and facial deficit + post-traumatic scar	Rhinoplasty	Lipostructure + 40% vol/vol PRP + insulin after 7, 15 days	No
34	M.P	39	F	No	Hemifacial atrophy + postsurgical scar	Removal angioma	Lipostructure + 40% vol/vol PRP + insulin after 7, 15 days	No
35	D.A	30	M	HCV+	Postburn scar	Skin expander + skin graft	Lipostructure + 40% vol/vol PRP + insulin after 7, 15 days	No
36	P.A	29	F	No	Breast postburn scar	Z-Plastic	Lipostructure + 40% vol/vol PRP + insulin after 7, 15 days	No
37	N.A	45	M	No	Postsurgical scar	Z-Plastic	Lipostructure + 40% vol/vol PRP + insulin after 7, 15 days	No
38	B.H	45	F	Diabetes	Hemifacial atrophy left	Poliglactac acid	Lipostructure + 40% vol/vol PRP + insulin after 7, 15 days	No
39	S.F	35	M	Romberg disease	Hemifacial atrophy right	No. 1 lipostructure	Lipostructure + 40% vol/vol PRP + insulin after 7, 15 days	No

^a Patients enclosed in a previous clinical study [20].

Abbreviations: HCV+, hepatitis C virus positive; PRP, platelet-rich plasma; Pt, patient.

Table 2. Primers used for reverse transcriptase-PCR and real-time PCR

Gene	Primer sequence	Accession number	Tann (°C)
<i>EGFR</i>	Sense 5'-GGGAAGAATGGGGTCGTCAA-3' Antisense 5'-CTCCTCCCTGGGGTGTCAAGT-3'	NM_005228	58
<i>ErbB2</i>	Sense 5'-TCTCAGGCAGTGTCTCTGG-3' Antisense 5'-CTCGAATCCACTGCAGGAAG-3'	NM_001005862	58
<i>ErbB3</i>	Sense 5'-TCTCAGGCAGTGTCTCTGG-3' Antisense 5'-CTCGAATCCACTGCAGGAAG-3'	NM_001982	58
<i>ErbB4</i>	Sense 5'-TGCCCTACAGAGCCCAACTA-3' Antisense 5'-GCTTGCGTAGGGTGCCATTAC-3'	NM_001042599	58
<i>FGFR-1</i>	Sense 5'-ATGTGTCTGCCCTCTATG-3' Antisense 5'-AAGCCAAGATCTGCGACAGT-3'	NM_001174064	58
<i>FGFR-2</i>	Sense 5'-CAGAGACCAACGTT CAAGCA-3' Antisense 5'-GAGGAAGGCATGGTTCTGTA-3'	NM_000141	58
<i>IR</i>	Sense 5'-TTATGCCCACTCCTTCAGG-3' Antisense 5'-CCAACACAGAGGTCCAAGGT-3'	NM_000208	58
<i>IGF1-R</i>	Sense 5'-AACCCCAAGACTGAGGTGTG-3' Antisense 5'-TGACATCTCTCCGCTTCCTT-3'	NM_000875	58
<i>MIG6</i>	Sense 5'-AGCCCTCTCTGGATGACA-3' Antisense 5'-CCAACAGCTTCTCCTTCTCG-3'	NM_018948	58
<i>PPARγ</i>	Sense 5'-TTCAGAAATGCCTTGCAAGT-3' Antisense 5'-CCAACAGCTTCTCCTTCTCG-3'	NM_005037	58
<i>β2m</i>	Sense 5'-GATTCAGGTTTACTCACGTC-3' Antisense 5'-GTTACACGGCAGGCATACT-3'	NM_004048	58
<i>CyPA</i>	Sense 5'-CATGGTCAACCCACCGTGTCTT-3' Antisense 5'-TAGATGGACTTGCCACCAGTGCCAT-3'	NM_021130	58
<i>GAPDH</i>	Sense 5'-ACGGATTTGGTCTGATTGG-3' Antisense 5'-GATTTTGGAGGGATCTCGC-3'	NM_002046	58

Abbreviations: PCR, polymerase chain reaction; Tann (°C), temperature of annealing.

Flow Cytometry

For flow cytometry, ASCs were labeled with mouse monoclonal anti-human CD90-PE and CD44-FITC (Santa Cruz Biotechnology, Santa Cruz, CA, <http://www.scbt.com>) on ice and protected from light for 30 minutes. At least 10,000 events were acquired on a FACSCalibur flow cytometer using CELLQuest acquisition software (Becton, Dickinson and Company, Franklin Lakes, NJ, <http://www.bd.com>) in triplicate.

Western Blot Analysis and Immunoprecipitation

After extraction and quantification of total cell lysates [25], proteins were separated by gradient sodium dodecyl sulfate-polyacrylamide gel electrophoresis, blotted to nitrocellulose transfer membranes, and incubated with anti-CD44 (Santa Cruz Biotechnology), anti-CD90 (Santa Cruz Biotechnology), anti-EGFR (Cell Signaling Technology, Beverly, MA, <http://www.cellsignal.com>), anti-ErbB3 (R&D Systems, Minneapolis, <http://www.rndsystems.com>), rabbit polyclonal anti-c-erbB-2 (Millipore, Billerica, MA, <http://www.millipore.com>), anti-phosphorylated ErbB2 (pTyr¹²⁴⁸) (Sigma-Aldrich), rabbit polyclonal anti-extracellular signal-regulated kinase (Erk1/2) (Cell Signaling Technology), rabbit monoclonal anti-phosphorylated Erk1/2 (phospho-Erk1/2, Cell Signaling Technology), rabbit monoclonal anti-Akt (pan) (C67E7, Cell Signaling Technology), rabbit monoclonal anti-phosphorylated-Akt (phospho-Akt Ser⁴⁷³) (193H12, Cell Signaling Technology), mouse monoclonal anti-sterol regulatory element binding protein-1 (SREBP-1) (2A4, BD Biosciences, Franklin Lakes, NJ, <http://www.bdbiosciences.com>), and anti- α -tubulin antibody (Sigma-Aldrich). Immunoprecipitation with anti-ErbB3 antibody (Abcam, Cambridge, U.K., <http://www.abcam.com>) was performed according to the manufacturer's guidelines using magnetic beads (Protein A Mag Sepharose, GE Healthcare Europe GmbH, Freiburg, Germany, <http://www.gehealthcare.com>). Densitometric blot analysis [25] was performed in three independent

experiments, and Akt and Erk1/2 activity was measured by phospho/total Akt and phospho/total Erk1/2 ratio.

Immunofluorescence

To verify stromal marker expression (supplemental online Figure 1), ASCs were fixed in 4% paraformaldehyde for 5 minutes at 4°C and then incubated with mouse monoclonal antibody anti-CD44 and anti-CD90 (Santa Cruz Biotechnology) and rabbit polyclonal anti-c-erbB-2 (Dako Cytomation, Glostrup, Denmark, <http://www.dako.com>) for 1 hour at room temperature. Specific secondary antibodies (Nordic Immunology, Tilburg, The Netherlands, <http://www.nordiclabs.nl>) were added, and then cells were incubated with fluorescent streptavidin (R&D Systems). Hoechst was used for nuclear staining.

Reverse Transcriptase and Real-Time Polymerase Chain Reaction

RNA extraction, reverse transcriptase-polymerase chain reaction (RT-PCR), and real-time PCR of cells and small residual adipose tissue volumes were performed as reported [26] using primer sequences for human ErbB receptors, fibroblast growth factor receptors 1 and 2 (*FGFR-1* and *FGFR-2*), insulin receptor (*IR*), insulin-like growth factor 1 receptor (*IGF1-R*), mitogen-induced gene 6 (*MIG6*), and peroxisome proliferator-activated receptor γ (*PPAR γ*) listed in supplemental online Table 2. Results were normalized on β -2-microglobulin, cyclophilin A, and glyceraldehyde-3-phosphate dehydrogenase transcript levels. Each experiment was performed in triplicate.

Statistical Analysis

Values as the mean + SE or SD were analyzed by means of Student's *t* test, and differences were considered statistically significant at $p < .05$. For three or more groups of univariate data, single-factor analysis of variation was used to obtain *p* values.

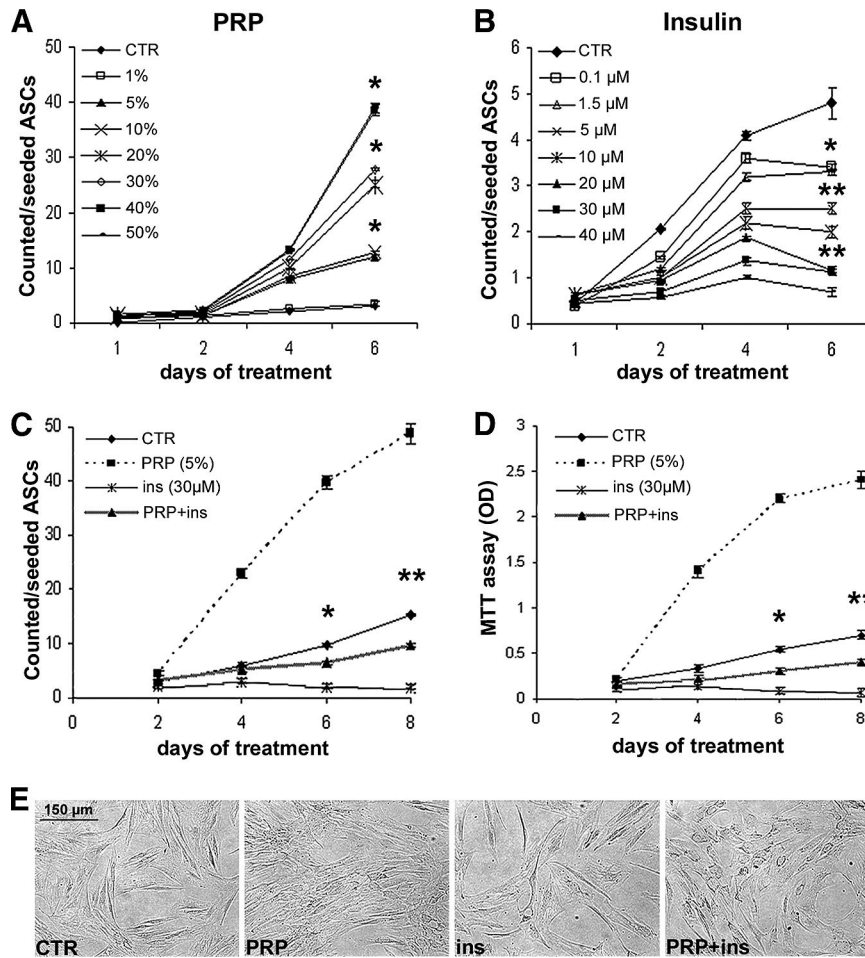


Figure 1. Effects of platelet-rich plasma and insulin on proliferation of human adipose-derived stem cells. **(A, B):** Growth curves show the dose-dependent increase of proliferation with PRP **(A)** and the dose-dependent reduction of proliferation with insulin **(B)** compared with serum-growth control ASCs. **(C, D):** The effect of PRP (5% vol/vol) and insulin (30 μM) alone and in combination on ASC proliferation **(C)** and cell viability **(D)** by MTT assay. Data are the mean ± SE. **(E):** Phase contrast micrographs of third passage cultured ASCs with 10% FBS as control or treated with PRP (5% vol/vol), insulin (30 μM) and the PRP-insulin combination. Scale bar = 150 μm. *, $p < .05$; **, $p < .01$. Abbreviations: ASCs, adipose-derived stem cells; CTR, control; ins, insulin; MTT, 3-(4,5-dimethylthiazole-2-yl)-2,5-diphenylterazolium bromide; OD, optical density; PRP, platelet-rich plasma.

RESULTS

Platelet-Rich Plasma and Insulin Exert Different Effects on Proliferation of ASCs

Growth curves (Fig. 1A) documented that PRP increased ASC proliferation in a dose-dependent manner ($EC_{50} = 15.3 \pm 1.3\%$ vol/vol), with a fourfold increase of cell number at 5% (vol/vol) dosage compared with control after 4 days (Fig. 1C, 1D; $p < .05$). Insulin treatment reduced proliferation in a dose-dependent manner ($IC_{50} = 3.0 \pm 0.46 \mu\text{M}$) when compared with control ASCs (Fig. 1B; $p < .01$). After 6 days, at higher concentrations insulin even reduced ASC number and viability compared with those after 4 days (Fig. 1B–1D). Insulin-induced cell loss was found to be associated with the increase of apoptotic figures by Hoechst (not shown). At 5% vol/vol dosage, PRP abolished insulin-induced antiproliferative effect and cell loss (Fig. 1C). Flow cytometry after 6 days (supplemental online Fig. 2A, 2B) documented that insulin, PRP, and PRP-insulin combination did not modify the percentage of CD90⁺ and CD44⁺ ASCs. Nevertheless, densitometric analysis (supplemental online Fig. 2C, 2D) showed a slight but significant increase of CD90 and CD44 protein con-

tent in PRP-insulin combination-treated compared with control ASCs ($p < .05$).

PRP Greatly Amplifies Insulin-Dependent Adipogenic Differentiation of ASCs

Quantification after Oil Red O staining (Fig. 2A, 2B) documented that, after PRP treatment, even with high dosages, intracytoplasmic lipid droplet accumulation was low and similar to serum control ASCs. Instead, insulin induced a dose-dependent lipid droplet accumulation in ASCs ($EC_{50} = 24.3 \pm 1.8 \mu\text{M}$; $p < .05$ at 30 μM versus control and 5% vol/vol PRP). Lipid droplet accumulation became visible after 3 days of treatment. Interestingly, PRP greatly amplified total and per-cell insulin-induced intracytoplasmic lipid accumulation at all examined concentrations. Ultrastructural examination (Fig. 2C) more clearly confirmed the increase in number and size of intracytoplasmic lipid droplets in PRP + insulin-treated ASCs. Finally, real-time PCR (Fig. 2D) showed an early increase of PPAR γ transcript level in insulin and, successively, in insulin + PRP-treated compared with control ASCs ($p < .01$ and $p < .05$, respectively). The difference in PPAR γ

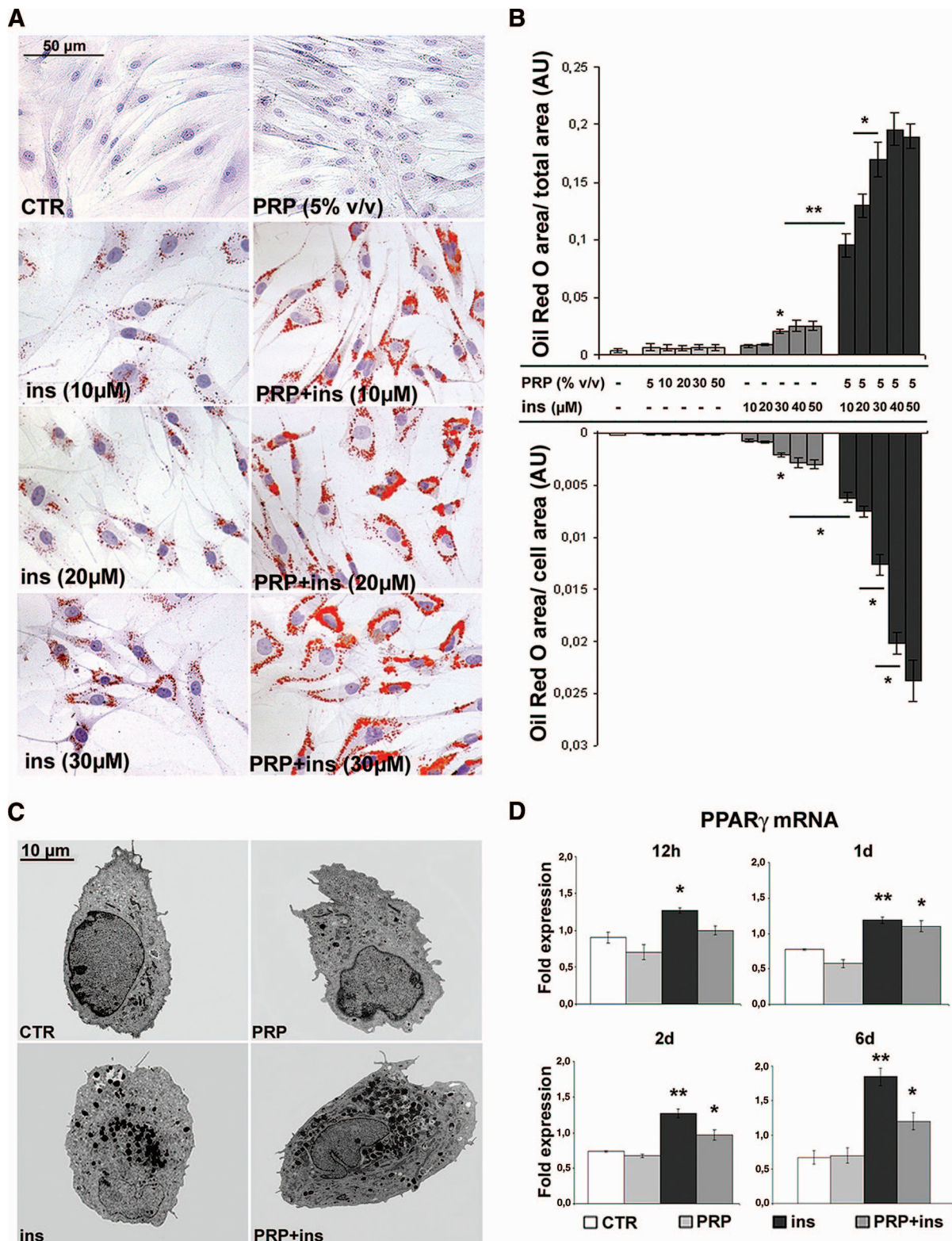


Figure 2. Effect of platelet-rich plasma and insulin on adipogenic differentiation of human adipose-derived stem cells. **(A):** Micrographs of Oil Red O-stained ASCs at third passage cultured in the presence of 10% fetal bovine serum (FBS), PRP (5% vol/vol), insulin (30 μ M), or the PRP-insulin combination for 6 days. Scale bar = 50 μ m. **(B):** Bar graph showing morphometric analysis after Oil Red O staining. Data are mean \pm SE. **(C):** Transmission electron microscopy images of 10% FBS control, PRP (5% vol/vol), insulin (30 μ M), and PRP + insulin-treated ASCs. Scale bar = 10 μ m. **(D):** Real-time polymerase chain reaction showing PPAR γ mRNA in control, PRP (5% vol/vol), insulin (30 μ M), and combined PRP + insulin-treated ASCs at different times. Data are mean \pm SD. *, $p < .05$; **, $p < .01$. Abbreviations: ASCs, adipose-derived stem cells; AU, arbitrary units; CTR, control; d, days; h, hours; ins, insulin; PPAR γ , peroxisome proliferator-activated receptor γ ; PRP, platelet-rich plasma.

transcript level of ASCs treated with insulin alone was greater than that of insulin + PRP at 6 days ($p < .05$).

Akt Activation Sustains PRP + Insulin-Induced Adipogenic Differentiation of ASCs

To clarify the mechanisms regulating ASC adipogenic differentiation, we investigated the role and modulation of Akt activity. As reported in Figure 3A and 3B, the 6-day treatment with PRP (5% vol/vol) associated with the reduction of Akt phosphorylation compared with control ASCs ($p < .01$), whereas with insulin alone phospho-Akt level did not vary. Instead, the combined PRP + insulin treatment induced a marked increase of Akt phosphorylation ($p < .01$), with no change in total Akt. Moreover, the PRP + insulin-induced Akt activity was accompanied by a significant increase of SREBP-1 accumulation ($p < .001$). The inhibition of Akt phosphorylation by wortmannin (Fig. 3C–3E) strongly reduced the PRP + insulin-induced intracytoplasmic lipid accumulation (~60%) and SREBP-1 expression ($p < .001$), supporting that Akt and Akt-regulated gene activity is required for adipogenic commitment of ASCs.

After the PRP + insulin treatment, Erk-1 ($p < .01$) but not Erk-2 activity was reduced compared with control ASCs (Fig. 3A, 3B), with no change in total Erk-1/2. Erk-1 activity was also variably reduced with PRP and insulin treatments ($p < .01$), suggesting that Erk-1 downregulation alone is not enough to modulate adipogenic differentiation of ASCs. The inhibition of phospho-Akt by wortmannin increased Erk activity in both control (Fig. 3C, 3D; $p < .01$) and PRP + insulin-treated ASCs ($p < .05$), confirming the hypothesis that the Erk-1 downregulation induced by PRP + insulin treatment is Akt dependent.

PRP Synergistically Upregulates FGFRs but Prevents Insulin-Induced IGF-1R and IR Downregulation

To clarify the cell signaling involved in Akt-dependent adipogenic differentiation of ASCs, we investigated the role of different receptors targeted by PRP and insulin. Real-time PCR documented that, after 6 days of combined PRP-insulin treatment of ASC, adipogenic differentiation was associated with a significant increase of FGFR-2 and less of FGFR-1 transcript levels (Fig. 3F; $p < .01$ and $p < .05$ versus control, respectively); FGFR-2 mRNA upregulation was already evident after 12 hours (supplemental online Fig. 3; $p < .01$). After 6 days of insulin treatment, IR and IGF-1R transcript levels were reduced compared with control ASCs (Fig. 3G, 3H; $p < .01$ versus control). In combination, PRP partially abolished the effects of insulin on IGF-1R and IR transcript levels.

FGFR-1 but Not FGFR-2 Inhibition Reduces Akt-Dependent Adipogenic Differentiation of ASCs

To better understand the role of FGFRs and/or IGF-1R in the adipogenic differentiation of ASCs, we specifically inhibited these receptors. As shown in Figure 4, the selective FGFR-1 inhibitor PD166866 reduced cell number and intracytoplasmic lipid accumulation (~30%) in PRP + insulin-treated compared with control ASCs (Fig. 4A–4C; $p < .05$ and $p < .001$, respectively). A similar reduction of cell number and lipid accumulation was observed with the total FGFR inhibitor PD173074, strongly suggesting that the inhibition of FGFR-2 activity affects ASC adipogenesis and proliferation minimally or not at all. Instead, IGF-1R selective inhibition did not modify ASC lipid accumulation and in combination did not amplify FGFR inhibitor effects. Fi-

nally, PD166866 inhibitor markedly inhibited Akt phosphorylation in control and in combined PRP + insulin-treated ASCs (Fig. 4D, 4E, $p < .001$ and $p < .01$, respectively). Similar effects were observed with PD173074 (data not shown). These findings support the crucial role of FGFR-1 signaling in Akt-dependent adipogenic commitment of ASCs.

PRP and Insulin Variably Modulated the Expression of ErbB Receptors

To further investigate the receptor pathways responsible for PRP and insulin-induced adipogenic differentiation, we investigated the expression of ErbB receptors. RT-PCR (Fig. 5A) documented higher EGFR, ErbB2, and ErbB4 transcript levels in adult human subcutaneous adipose tissue rather than in serum-cultured ASCs. Unlike adult adipose tissue, ASCs expressed detectable ErbB3 mRNA. Real-time PCR documented that, during the first 2 days of treatment, when lipid droplet accumulation was not yet visible, the EGFR transcript level was slightly downregulated in insulin + PRP-treated ASCs (supplemental online Fig. 4; $p < .05$). Successively, blots and real-time PCR (Fig. 5B and supplemental online Fig. 4) documented that the 6-day insulin treatment was associated with the marked increase of EGFR expression ($p < .05$ versus control). Interestingly, PRP alone reduced EGFR expression and, in combination, completely reversed the effects of insulin. During the first days of treatment, insulin and PRP slightly downregulated ErbB2 transcript level (supplemental online Fig. 4; $p < .05$ versus control ASCs). After 6 days, insulin treatment was found to be associated with the strong increase of ErbB2 expression and activity as detected by phospho-ErbB2 expression (Fig. 5C, 5D, and supplemental online Fig. 4; $p < .01$ and $p < .05$ versus control, respectively). PRP exerted the opposite action, completely reversed the effects of insulin, and strongly reduced the expression and activity of ErbB2 (Fig. 5C). Interestingly, the PRP-insulin combination initially increased MIG6 mRNA, whereas successively it prevented the marked MIG6 downregulation observed with insulin alone after 6 days (supplemental online Fig. 4; $p < .01$ versus control). After 6 days, PRP and insulin both reduced ErbB3 expression compared with control ASCs (Fig. 5E, 5F; $p < .05$), and the effect was cumulative ($p < .01$). Blots and immunoprecipitation (not shown) also documented the presence of ErbB3 truncated forms of ~75, 37, ~30, and 25 kDa. Insulin alone and in combination with PRP downregulated 37 and 25 kDa ErbB3 truncated forms ($p < .05$), whereas the addition of PRP reversed insulin-induced 25 kDa truncated form reduction ($p < .05$). Finally, PRP initially downregulated the ErbB4 transcript level, and after 6 days this effect was found when using insulin in the combined treatment (supplemental online Fig. 4).

EGFR and ErbB2 Activities Differently Influence Proliferation and Adipogenic Differentiation of ASCs

We also investigated, by using specific inhibitors, the influence of EGFR and ErbB2 activity in the modulation of proliferation and adipogenic commitment of ASCs. As reported in Figure 6A and 6B, the selective inhibitors of EGFR, AG1478, and of ErbB2, AG879, both induced an antiproliferative effect in all experimental conditions when compared with control ASCs. AG879 ($IC_{50} = 3.6 \pm 0.5 \mu M$) was more effective than AG1478 ($IC_{50} = 6.33 \pm 0.8 \mu M$). Interestingly, the antiproliferative effect of AG1478 and AG879 was not cumulative (Fig. 6C). EGFR and ErbB2 inhibitors

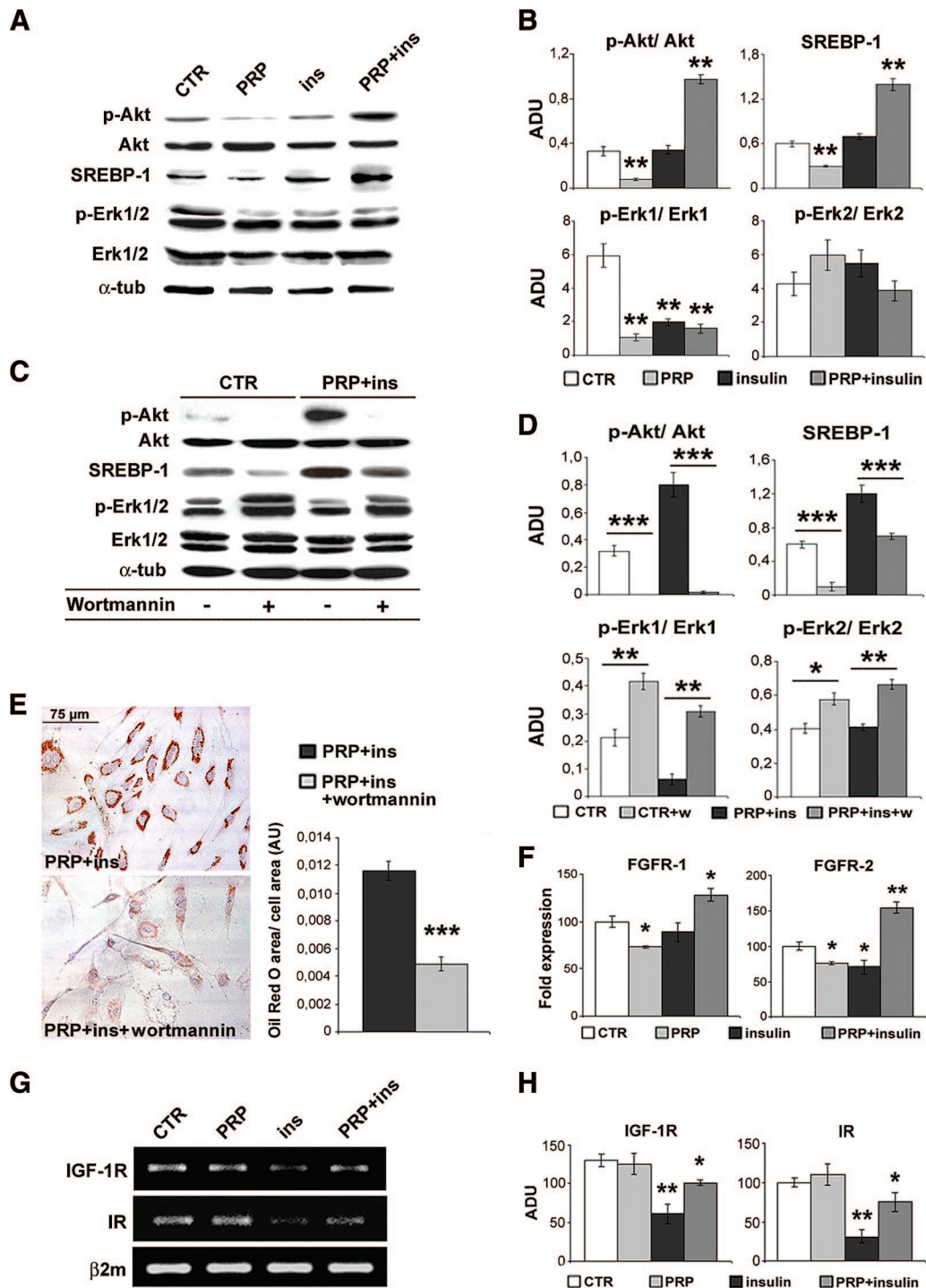


Figure 3. Effect of platelet-rich plasma and insulin on Akt and Erk1/2 activity and FGFR, IGF-1R, and IR transcript levels in human adipose-derived stem cells. **(A, B):** Representative blot **(A)** and densitometric analysis **(B)** of phosphorylated and total Akt, SREBP-1, and phosphorylated and total Erk1/2 in control, PRP (5% vol/vol), insulin (30 μ M), and PRP + insulin-treated ASCs after 6 days. Data are mean \pm SE. **(C, D):** Representative blot **(C)** and densitometric analysis **(D)** of phosphorylated and total Akt, SREBP-1, and phosphorylated and total Erk1/2 expression in control and PRP + insulin with or without Akt inhibitor wortmannin (10 μ M) for 6 days. Data are mean \pm SE. **(E):** Micrographs of Oil Red O staining and morphometric analysis of third passage ASCs cultured with PRP (5% vol/vol) + insulin (30 μ M) in the presence of 10% fetal bovine serum and wortmannin (10 μ M) for 6 days. Scale bar = 75 μ m. Data are mean \pm SE. **(F):** Real-time polymerase chain reaction (PCR) showing FGFR-1 and FGFR-2 mRNA in control, PRP (5% vol/vol), insulin (30 μ M), and combined PRP + insulin-treated ASCs after 6 days. Data are mean \pm SE. **(G, H):** Reverse transcriptase PCR **(G)** and densitometric analysis **(H)** documenting IGF-1R and IR transcripts in serum control, PRP (5% vol/vol), insulin (30 μ M), and PRP + insulin-treated ASCs after 6 days. Data are mean \pm SE. *, $p < .05$; **, $p < .01$; ***, $p < .001$. Abbreviations: ADU, arbitrary densitometric units; α -tub, α -tubulin; AU, arbitrary units; β 2m, β -2-microglobulin; CTR, control; FGFR-1, fibroblast growth factor receptor-1; FGFR-2, fibroblast growth factor receptor-2; IGF-1R, insulin-like growth factor-1 receptor; ins, insulin; IR, insulin receptor; p-Akt, phosphorylated Akt; p-Erk1/2, phosphorylated Erk1/2; PRP, platelet-rich plasma; SREBP, mouse monoclonal anti-sterol regulatory element binding protein-1; w, wortmannin.

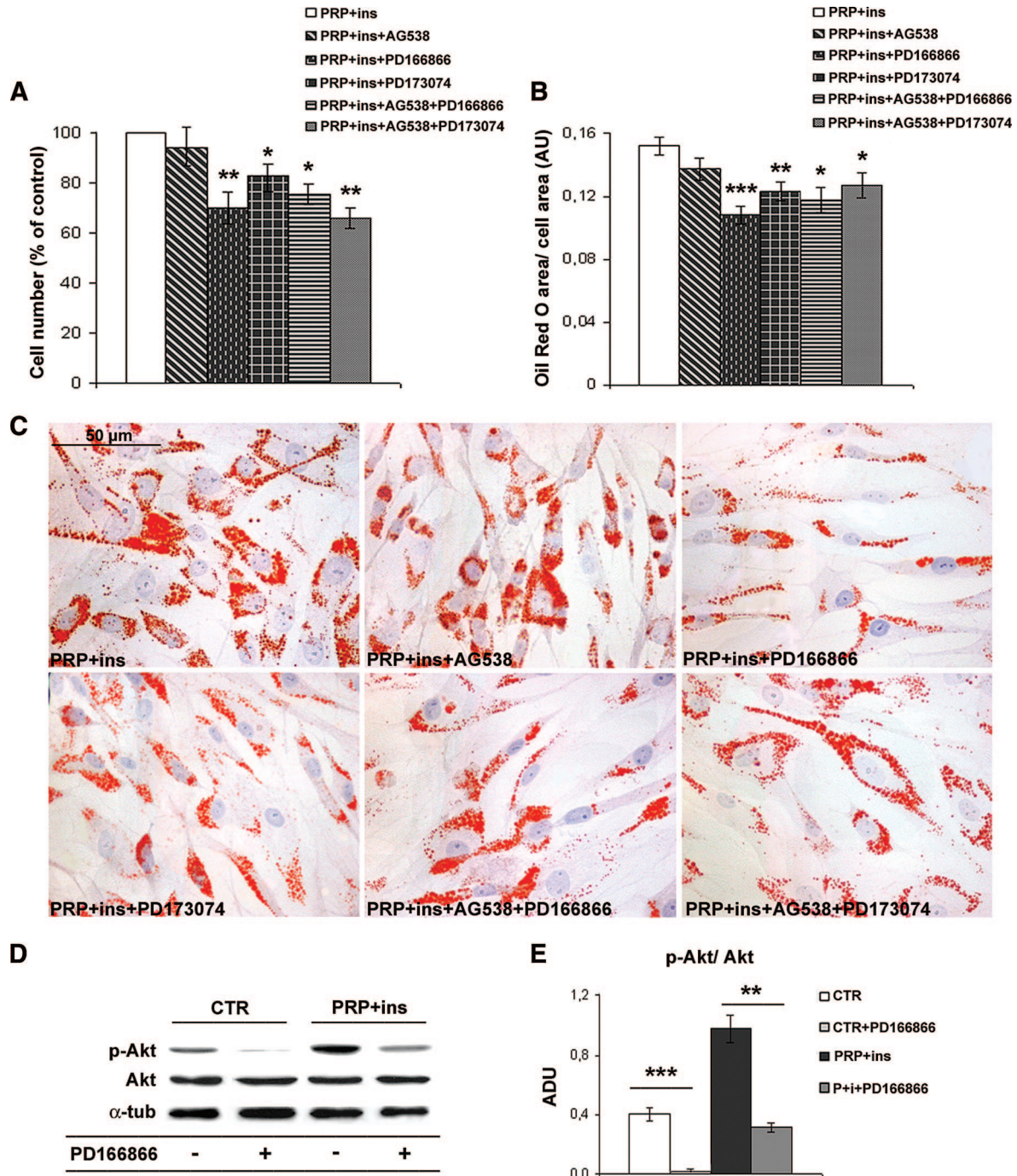


Figure 4. Effects of specific fibroblast growth factor receptors and insulin-like growth factor receptor inhibitors on proliferation, adipogenic differentiation, and Akt phosphorylation in human adipose-derived stem cells. **(A, B):** Bar graphs showing cell number and intracytoplasmic lipid accumulation of ASCs after 6 days of exposition to PD166866 (100 nM), PD173074 (50 nM), and AG538 (10 μ M) in the presence of 10% fetal bovine serum (FBS), PRP (5% vol/vol), and insulin (30 μ M). Data are mean \pm SE. **(C):** Representative Oil Red O staining micrographs of third passage ASCs treated with PD166866 (100 nM), PD173074 (50 nM), and AG538 (10 μ M) in the presence of 10% FBS, PRP (5% vol/vol), and insulin (30 μ M) for 6 days. Scale bar = 50 μ m. **(D, E):** Representative blot **(D)** and densitometric analysis **(E)** of phosphorylated and total Akt expression in control, PRP + insulin, and FGFR-1 inhibitor (100 nM PD166866)-treated ASCs after 6 days. Data are mean \pm SE. *, $p < .05$; **, $p < .01$; ***, $p < .001$. Abbreviations: ADU, arbitrary densitometric units; α -tub, α -tubulin; AU, arbitrary units; CTR, control; ins, insulin; p-Akt, phosphorylated Akt; PRP, platelet-rich plasma.

influenced differently intracytoplasmic lipid droplet accumulation. As reported in Figure 6D and 6E, although the proliferation rate was similar but slightly reduced, after 6 days at 5 μ M concentration AG879 markedly increased lipid droplet accumulation

in both control and in PRP + insulin-treated ASCs ($p < .01$), whereas the AG1478 effect was slightly depleting. Together, these findings suggest that ErbB2 activity regulates proliferation and adipogenic commitment of ASCs through two independent

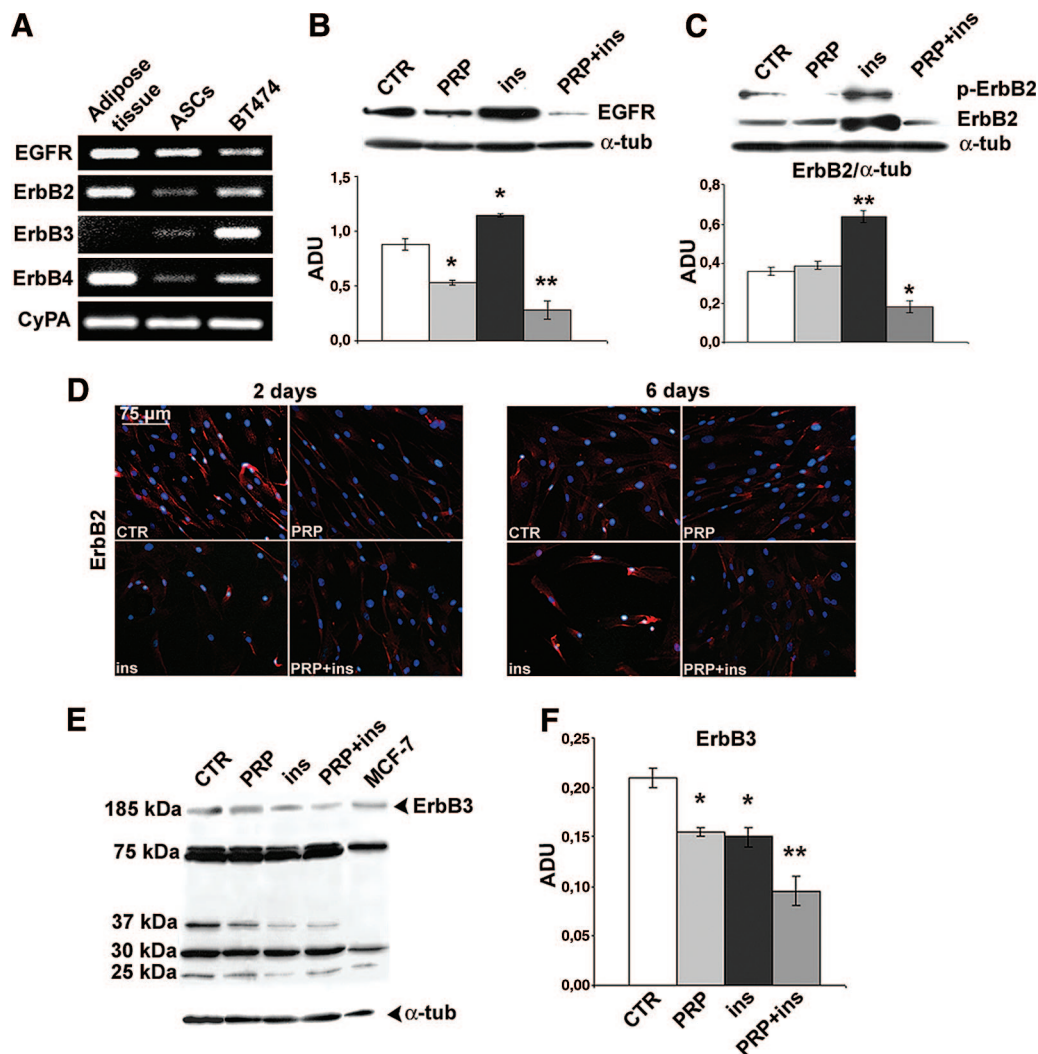


Figure 5. Effect of platelet-rich plasma and insulin on ErbB receptor expression during adipogenic differentiation of human adipose-derived stem cells. **(A):** ErbB receptor transcript levels in human subcutaneous adipose tissue, human ASCs by reverse transcriptase polymerase chain reaction; BT474 breast cancer cell line is the positive control. **(B):** Representative blot and densitometric analysis of EGFR expression in ASCs after PRP (5% vol/vol), insulin (30 μ M), and the PRP-insulin combination treatment after 6 days. Data are mean \pm SE. **(C):** Western blot and densitometric analysis of total ErbB2 and phospho-ErbB2 in ASCs after PRP (5% vol/vol), insulin (30 μ M), and combined PRP + insulin treatment after 6 days. **(D):** ErbB2 expression in serum control, PRP (5% vol/vol), insulin (30 μ M), and combined PRP + insulin-treated ASCs by immunofluorescence after 2 and 6 days. Scale bar = 75 μ m. **(E, F):** Representative blot **(E)** and densitometric analysis **(F)** of ErbB3 in PRP (5% vol/vol), insulin (30 μ M), and PRP + insulin-treated ASCs after 6 days; MCF-7 breast cancer cell line is the positive control. Data are mean \pm SE. *, $p < .05$; **, $p < .01$; ***, $p < .001$. Abbreviations: ADU, arbitrary densitometric units; ASCs, adipose-derived stem cells; α -tub, α -tubulin; CTR, control; CyPA, cyclophilin A; EGFR, epidermal growth factor receptor; ErbB, epidermal growth factor receptor; ins, insulin; p-ErbB2, phosphorylated ErbB2; PRP, platelet-rich plasma.

pathways. In combination, AG1478 partially abolished AG879-induced ASC intracytoplasmic lipid accumulation and partially prevented insulin + PRP-sustained adipogenesis (Fig. 6D, 6E). Finally, AG879 inhibitor increased Akt phosphorylation in control and in PRP + insulin-treated ASCs (Fig. 6F, 6G; $p < .05$). These data suggest that ErbB2 activity contributes to inhibit Akt phosphorylation and confirm the main role of Akt pathway during adipogenic differentiation of ASCs.

The Combination of PRP and Insulin Improves Clinical Long-Term Fat Graft Maintenance

We investigated the effects of the combination PRP and insulin on long-term fat graft maintenance in patients who underwent

surgery correction of soft tissue defects. As reported in Figure 7A, PRP induced the increase of clinical maintenance of three-dimensional volume of fat graft up to 40% vol/vol dosage. Insulin injection induced an increase of contour restoring and three-dimensional volume maintenance of fat graft compared with patients with PRP alone starting from a 12-week follow-up (Fig. 7B, $p < .01$). We also documented an absence of irregularity and dyschromia after 3- and 6-week follow-ups in patients with fat grafting plus PRP and insulin compared with those with fat graft plus PRP alone, as well as the reduced percentage of asymmetry and deformity after 24 and 52 weeks (Fig. 7C). In Figure 7D and 7E, the comparison between pre- and postoperative photos and magnetic resonance imaging of a patient treated with fat graft plus PRP and insulin is shown.

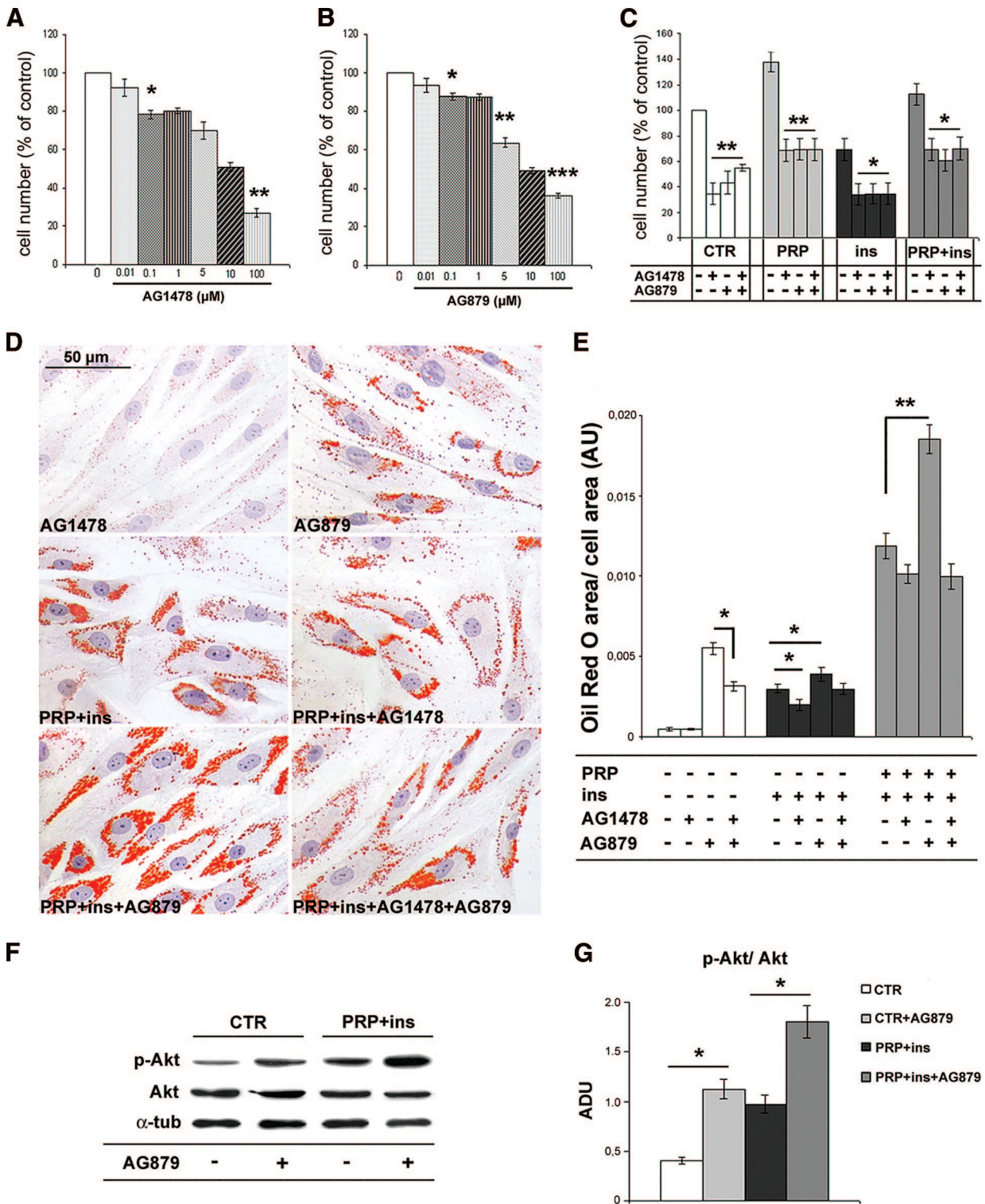


Figure 6. Effects of epidermal growth factor receptor (EGFR) and epidermal growth factor receptor 2 (ErbB2) inhibition on proliferation, adipogenic differentiation, and Akt phosphorylation in human adipose-derived stem cells (ASCs). **(A–C):** Bar graphs showing the dose-dependent inhibition of ASC proliferation after 48 hours of exposition to AG1478 and AG879, EGFR and ErbB2 selective inhibitors, respectively, in the presence of 10% fetal bovine serum. Data are mean ± SE. **(D):** Representative Oil Red O staining micrographs of third passage ASCs treated with AG1478 (5 μM), AG879 (5 μM), PRP (5% vol/vol), and insulin (30 μM) alone and in combination for 6 days. Scale bar = 50 μm. **(E):** Bar graph showing morphometric intracytoplasmic lipid quantification of Oil Red O-stained ASCs after the treatment with ErbB inhibitors. Data are mean ± SE. **(F, G):** Representative blot **(F)** and densitometric analysis **(G)** of phosphorylated and total Akt expression in control, PRP + insulin, and ErbB inhibitor AG879 (5 μM)-treated ASCs after 6 days. Data are mean ± SE. *, *p* < .05; **, *p* < .01; ***, *p* < .001. Abbreviations: ADU, arbitrary densitometric units; α-tub, α-tubulin; AU, arbitrary units; CTR, control; ins, insulin; p-Akt, phosphorylated Akt; PRP, platelet-rich plasma.

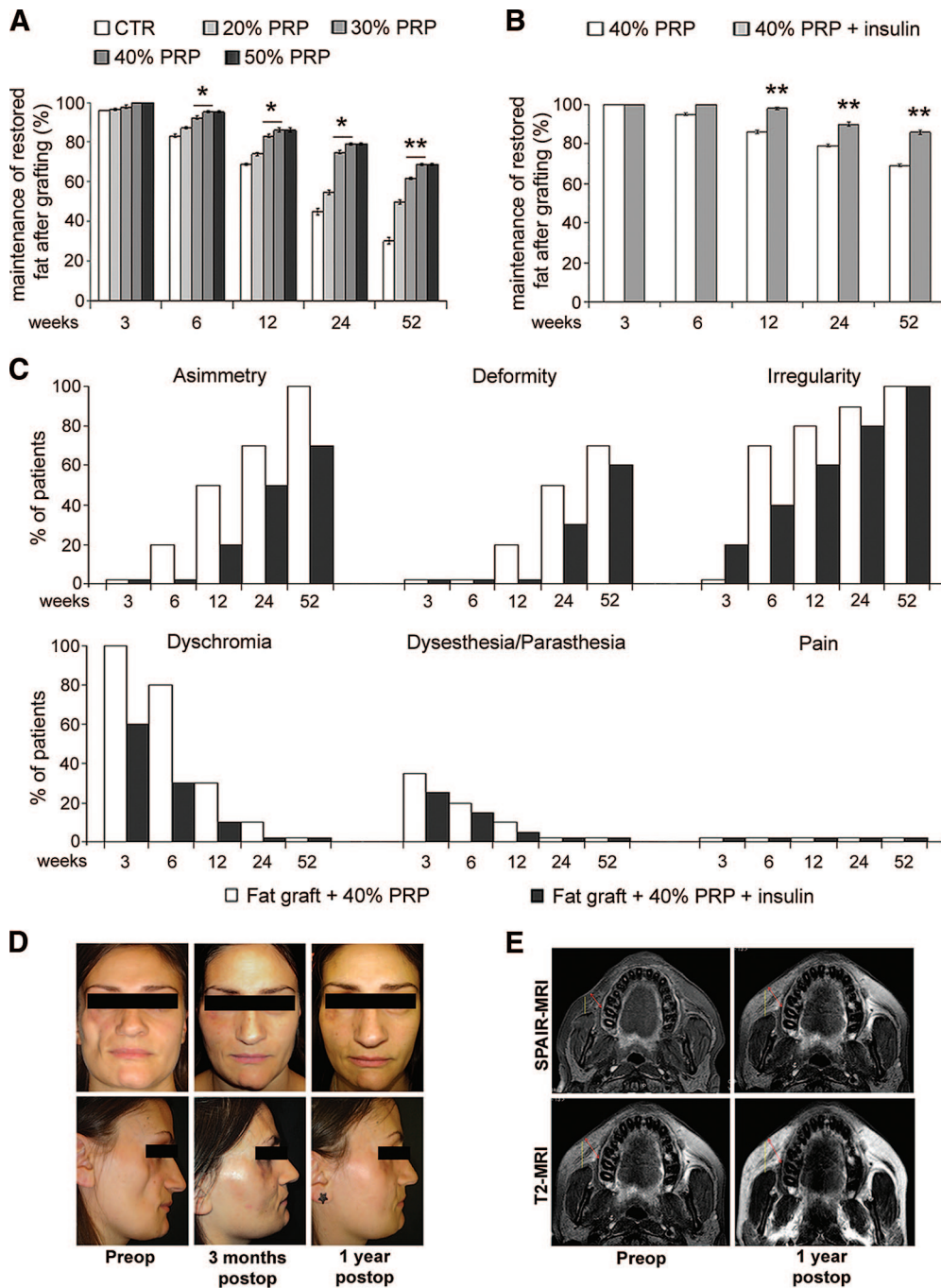


Figure 7. Clinical evaluation of the effects of platelet-rich plasma and insulin injection on long-term human fat graft maintenance. **(A):** Bar graph showing the percentage of restored fat graft volume maintenance with different PRP concentrations after 3, 6, 12, 24, and 52 weeks. **(B):** Bar graph showing the percentage of restored fat graft maintenance in patients treated with fat graft + 40% vol/vol PRP and the local injection of 0.5 ml human recombinant insulin (40 μM) performed 7 and 15 days after grafting in comparison with patients receiving fat graft + 40% PRP vol/vol alone. **(C):** Bar graphs showing the different percentages of patients presenting symptoms and sign default at different times after the treatment with fat graft + 40% vol/vol PRP alone or plus insulin injection. Data are mean ± SE. **(D):** Pre- and postoperative photos of a patient treated with fat graft + 40% PRP + insulin. **(E):** Pre- and postoperative spectral selection attenuated inversion recovery-magnetic resonance imaging and T2-MRI of the same patient. *, ** indicate $p < .05$ and $p < .01$, respectively. Abbreviations: CTR, control; PRP, platelet-rich plasma; preop, preoperative; postop, postoperative; SPAIR-MRI, spectral selection attenuated inversion recovery-magnetic resonance imaging; T2-MRI, T2-weighted-magnetic resonance imaging.

DISCUSSION

In this study, we documented the positive and potent synergism of PRP and insulin on adipogenic differentiation of human sub-

cutaneous ASCs and on clinical maintenance of fat grafting. It has been reported that PRP stimulated the rapid growth of ASCs without loss of differentiative potential capacity and stem marker expression [17, 19]. PRP also promotes proliferation of

human periodontal ligament and mesenchymal stem cells [27, 28]. PRP-sustained proliferation of ASCs was found to be associated with no significant change of intracytoplasmic lipid accumulation, as reported [20]. Instead, insulin induced a slight but significant dose-dependent increase of lipid accumulation parallel to PPAR γ mRNA upregulation in ASCs. This adipogenic role of insulin is in accordance with previous findings [21, 22] and is also reported in rat adipose-derived stromal cells, with some differences between adipogenic and mitogenic effect [29]. Unfortunately, insulin-induced adipogenic differentiation of ASCs associated to the reduced growth compared with serum control and even cell loss in long-term cultures. Insulin-induced apoptotic cell loss has also been described in rat brown adipose tissue [30]. Proliferative arrest and/or cell loss are potential limitations to regenerative medicine strategies, where growth factors should provide the necessary microenvironmental signals to accelerate tissue deposition from cell proliferation and matrix synthesis [10]. Here we documented that the addition of PRP greatly amplifies (up to 8 times) the insulin-induced intracytoplasmic lipid accumulation and prevents the proliferative arrest and/or apoptosis of ASCs. Because PRP alone did not increase significantly intracytoplasmic lipid accumulation in ASCs, its potent adipogenic effect in combination with insulin can be explained only in part with the reported adipogenic properties of some of its delivered growth factors [31, 32]. In this light b-FGF, which is abundantly contained in PRP, improved adipogenic differentiation induced by hormonal cocktail including insulin [33]. As concerning the pathways activated during PRP + insulin-sustained adipogenic differentiation of ASCs, we documented a strong increase of Akt activity much greater than with insulin alone, which was not observed with PRP alone. Conversely, PRP + insulin-induced intracytoplasmic lipid accumulation was greatly impaired by the Akt inhibitor wortmannin. The relevance of Akt in adipogenic differentiation of ASCs was also described in murine 3T3-L1 preadipocytes [24, 34]. Akt contributes to regulate significantly survival, proliferation, and metabolism in response to many cellular stimuli, including growth factors [23]. Mouse embryonic fibroblasts lacking Akt are unable to differentiate into adipocytes [35]. Moreover, Akt contributes to the synthesis of new lipids for cell membrane building by increasing cytosolic acetyl-CoA availability [36]. Akt activation stimulates glucose uptake in response to insulin [23] and inhibits hepatocyte glucose conversion, gluconeogenesis, and fatty acid oxidation [37], likely favoring intracellular lipid accumulation. The SREBP family of transcription factors control cholesterol and lipid metabolism and play a critical role during adipocyte differentiation [38]. We documented that SREBP-1 accumulation was parallel to that of Akt and intracytoplasmic lipid storage, suggesting that the Akt-regulated activation of SREBP-1 gene sustains lipid biosynthesis in ASCs [39]. We also observed that PRP + insulin-induced proliferation associated to the reduction of Erk-1 activity compared with insulin alone. Akt-induced inhibition of Erk pathway is also reported in other cell types, including myoblasts [40]. PRP and insulin synergistically markedly reduced phospho-Erk1 but not phospho-Erk2. Erk signaling has been reported to antagonize 3T3-L1 adipogenic gene profile expression [41]. Because Erk-1 sustains cell mitotic clonal expansion, it is likely that Erk-1 signal transduction pathway needs to be shut off to allow adipogenic differentiation [42].

We investigated the receptor signaling involved in PRP + insulin-induced Akt activation and adipogenesis of ASCs. FGFR-1 belongs to a family of receptor protein tyrosine kinases [43]. We

documented that only in combination PRP and insulin strongly increased FGFR mRNA. Nevertheless, the selective inhibition of FGFR-1 reduced intracytoplasmic lipid droplet accumulation and Akt phosphorylation at the same level of total FGFR inhibitor, strongly supporting the main involvement of FGFR-1 signaling in adipogenic commitment of ASCs. FGFR-1 signaling is mediated via direct recruitment of FGF ligands that bind to tyrosine autophosphorylation sites on the activated FGFR-1, resulting in activation of the Akt pathway responsible for cell differentiation and proliferation [43].

To further analyze the complex signaling that modulates ASC proliferation and adipogenesis, we investigated the expression of the ErbB tyrosine kinase receptor family. The latter regulate several cell biology processes, including proliferation, survival, differentiation, and tumorigenesis [44]. Some works documented the involvement of ErbB receptors in 3T3-L1 adipogenesis [45, 46]. PRP alone induced the slight downregulation of EGFR and the marked reduction of expression and activity of ErbB2 in ASC cultures, whereas insulin induced the opposite effects. The enhanced adipogenic differentiation of ASCs after PRP + insulin treatment was parallel to the robust downregulation of the expression and activity of EGFR and ErbB2, as also reported in murine 3T3-L1 pre-adipocytes stimulated to differentiate by dexamethasone and isobutyl methylxanthine [47]. Moreover, PRP + insulin-induced downregulation of ErbB2 preceded visible lipid droplet accumulation [45]. Similarly, ErbB2 inhibition increased intracytoplasmic lipid accumulation and up-regulated Akt phosphorylation, whereas EGFR inhibition induced the opposite effects. These findings document that the modulation of ErbB2 contributes to the adipogenic differentiation of ASCs. Nevertheless, in combination EGFR inhibitor partially prevented adipogenic effects of ErbB2 inhibitor, supporting that the inhibition of EGFR activity accounts for ErbB2 transinactivation [48]. In fact, although ErbB2 is unable to interact directly with EGF ligands, ErbB2 forms heterodimers with other ErbB receptors, which contribute to generate intracellular signals [44]. EGFR and ErbB2 activation is critically regulated by the intracellular kinase domain that is inhibited by the interaction with the cytoplasmic protein MIG6 [49]. PRP in combination with insulin initially upregulated and successively completely abolished the late reduction of MIG6 transcription induced by insulin alone, suggesting that MIG6 upregulation downregulates ErbB2 and favors the subsequent lipid accumulation in ASCs. A similar effect on MIG6 mRNA is reported with IGF-1, a component of PRP, in mouse brown preadipocytes [50], supporting that the complex regulatory scenario of ASC adipogenic differentiation is maintained in vivo. Differently from adult adipose tissue, ASCs significantly expressed ErbB3 transcripts. PRP and insulin synergistically downregulated the expression of ErbB3, which displays a defective kinase activity [44]. Insulin-dependent reduction of ErbB3 binding activity has been previously reported in other cell types [51]. We also documented the presence of different ErbB3 truncated forms, and PRP also partially prevented insulin-induced modulation of 25 and 37 kDa ErbB3 truncated forms. The latter have been previously reported in normal human tissues and tumor-derived cell lines [52], but further studies are needed to explore a functional role during ASC adipogenesis.

In recent years, experiments aimed at developing new methods of improving adipose tissue transplantation efficacy received substantial acceleration. The ultimate goal is to improve the

maintenance of long-term graft volume and viability and to reduce adverse inflammatory response [53]. Although the use of autologous adipose tissue provides the benefit of lowering the risk of immunogenic response and the absence of potential pathogen transfers, the clinical success of fat grafting is limited by a variable and unpredictable low survival rate [7]. PRP has been introduced in many fields of regenerative surgery [12, 13] and improves long-term fat graft maintenance [20]. We documented that the PRP-insulin combination further improves long-term fat graft volume maintenance and contour restoring in patients with tissue defects compared with PRP alone. Although additional studies are needed, our data strongly support that PRP-induced sustained proliferation and amplification of insulin-dependent adipogenic commitment of ASCs contribute to this clinical advantage. An indirect confirmation derives from the finding that experimental insulin delivery in the deep muscular fascia of the rat abdominal wall induced adipose tissue generation from differentiation of nonadipocyte cells, rather than from the increase in size of preexisting adipocytes [22]. Finally, preliminary studies document that SVF enrichment improves wound healing [54, 55] and that ASCs can be successfully transplanted for regenerative surgery [56]. Large clinical trials and a careful follow-up are needed to better explore safety and efficacy of SVF/ASC enrichment.

CONCLUSION

We documented that PRP in combination prevents insulin-induced proliferation arrest and greatly potentiates adipogenic

differentiation in human ASCs. PRP + insulin sustained activities of Akt and Akt downregulated genes, such as SREBP-1 and MIG-6, appear crucial for the adipogenic differentiation of ASCs, and FGFR-1 and ErbB2 signaling plays a pivotal role in Akt activation (supplemental online Fig. 5). The amelioration of long-term maintenance in patients undergoing fat grafting procedures for soft tissue defects strongly supports that the positive synergistic effect of PRP and insulin is maintained in vivo. These findings suggest additional beneficial therapeutic opportunities of the association of PRP and insulin in other fields of regenerative medicine.

ACKNOWLEDGMENTS

This work was partially supported from a grant from Transplantation Agency of Lazio, Rome, Italy. We thank Sabrina Cappelli and Antonio Volpe for their valuable technical collaboration.

AUTHOR CONTRIBUTIONS

V.C., L.G.S.: conception and design, data analysis and interpretation; M.G.S.: conception and design, collection and assembly of data, data analysis and interpretation; P.G., E.D., E.B.: collection and assembly of data; A.O.: conception and design, financial support, administrative support, provision of study material, data analysis and interpretation, writing and final approval of the manuscript.

REFERENCES

- Williams DF. To engineer is to create: The link between engineering and regeneration. *Trends Biotechnol* 2006;24:4–8.
- Peterson B, Zhang J, Iglesias R et al. Healing of critically sized femoral defects, using genetically modified mesenchymal stem cells from human adipose tissue. *Tissue Eng* 2005; 11:120–129.
- Oedayrajasingh-Varma MJ, van Ham SM, Knippenberg M et al. Adipose tissue-derived mesenchymal stem cell yield and growth characteristics are affected by the tissue-harvesting procedure. *Cytotherapy* 2006;8: 166–177.
- Prunet-Marcassus B, Cousin B, Caton D et al. From heterogeneity to plasticity in adipose tissues: Site-specific differences. *Exp Cell Res* 2006;312:727–736.
- McIntosh K, Zvonic S, Garrett S et al. The immunogenicity of human adipose-derived cells: Temporal changes in vitro. *STEM CELLS* 2006;24:1246–1253.
- Mitchell JB, McIntosh K, Zvonic S et al. Immunophenotype of human adipose-derived cells: Temporal changes in stromal-associated and stem cell-associated markers. *STEM CELLS* 2006;24:376–385.
- Coleman SR. Structural fat grafting: More than a permanent filler. *Plast Reconstr Surg* 2006;118:1085–1205.
- Locke MB, de Chalmers TM. Current practice in autologous fat transplantation: Suggested clinical guidelines based on a review of recent literature. *Ann Plast Surg* 2008;60:98–102.
- Eppley BL, Pietrzak WS, Blanton M. Platelet-rich plasma: A review of biology and applications in plastic surgery. *Plast Reconstr Surg* 2006;118:147e–159e.
- Chen FM, Zhang M, Wu ZF. Toward delivery of multiple growth factors in tissue engineering. *Biomaterials* 2010;62:79–6308.
- Nurden AT, Nurden P, Sanchez M et al. Platelets and wound healing. *Front Biosci* 2008;13:3532–3548.
- Whitman DH, Berry RL, Green DM. Platelet gel: An autologous alternative to fibrin glue with applications in oral and maxillofacial surgery. *J Oral Maxillofac Surg* 1997;55:1294–1299.
- Margolis DJ, Kantor J, Santanna J et al. Effectiveness of platelet releasate for the treatment of diabetic neuropathic foot ulcers. *Diabetes Care* 2001;24:483–488.
- Mazzucco L, Balbo V, Cattana E et al. Not every PRP-gel is born equal. Evaluation of growth factor availability for tissues through four PRP-gel preparations: Fibrinet, regenPRP-Kit, plateltex and one manual procedure. *Vox Sang* 2009;97:110–118.
- Liu Y, Kalen A, Risto O et al. Fibroblast proliferation due to exposure to a platelet concentrate in vitro is pH dependent. *Wound Repair Regen* 2002;10:336–340.
- Gonzalez AM, Loboocki C, Kelly CP et al. An alternative method for harvest and processing fat grafts: An in vitro study of cell viability and survival. *Plast Reconstr Surg* 2007;120:285–294.
- Kakudo N, Minakata T, Mitsui T et al. Proliferation-promoting effect of platelet-rich plasma on human adipose-derived stem cells and human dermal fibroblasts. *Plast Reconstr Surg* 2008;122:1352–1360.
- Koellensperger E, von Heimburg D, Markowicz M et al. Human serum from platelet-poor plasma for the culture of primary human preadipocytes. *STEM CELLS* 2006;24:1218–1225.
- Kocaoemer A, Kern S, Kluter H et al. Human AB serum and thrombin-activated platelet-rich plasma are suitable alternatives to fetal calf serum for the expansion of mesenchymal stem cells from adipose tissue. *STEM CELLS* 2007; 25:1270–1278.
- Cervelli V, Gentile P, Scioli MG et al. Application of platelet-rich plasma in plastic surgery: Clinical and in vitro evaluation. *Tissue Eng Part C Methods* 2009;15:625–634.
- Wabitsch M, Hauner H, Heinze E et al. The role of growth hormone/insulin-like growth factors in adipocyte differentiation. *Metabolism* 1995;44:45–49.
- Yuksel E, Weinfeld AB, Cleek R et al. De novo adipose tissue generation through long-term, local delivery of insulin and insulin-like growth factor-1 by PLGA/PEG microspheres in an in vivo rat model: A novel concept and capability. *Plast Reconstr Surg* 2000;105:1721–1729.
- Manning BD CL. AKT/PKB signaling: Navigating downstream. *Cell* 2007;129:1261–1274.
- Bhattacharya I, Ullrich A. Endothelin-1 inhibits adipogenesis: Role of phosphorylation of Akt and ERK1/2. *FEBS Lett* 2006;580:5765–5771.

- 25 Orlandi A, Francesconi A, Marcellini M et al. Propionyl-L-carnitine reduces proliferation and potentiates Bax-related apoptosis of aortic intimal smooth muscle cells by modulating nuclear factor-kappaB activity. *J Biol Chem* 2007;282:4932–4942.
- 26 Stasi MA, Scioli MG, Arcuri G et al. Propionyl-L-carnitine improves postischemic blood flow recovery and arteriogenic revascularization and reduces endothelial NADPH-oxidase 4-mediated superoxide production. *Arterioscler Thromb Vasc Biol* 2010;30:426–435.
- 27 Han J, Meng HX, Tang JM et al. The effect of different platelet-rich plasma concentrations on proliferation and differentiation of human periodontal ligament cells in vitro. *Cell Prolif* 2007;40:241–252.
- 28 Mishra A, Tummala P, King A et al. Buffered platelet-rich plasma enhances mesenchymal stem cell proliferation and chondrogenic differentiation. *Tissue Eng Part C Methods* 2009;15:431–435.
- 29 Sadie-Van Gijsen H, Crowther NJ, Hough FS et al. Depot-specific differences in the insulin response of adipose-derived stromal cells. *Mol Cell Endocrinol* 2010;328:22–27.
- 30 Korac A, Radovanovic J, Davidovic V et al. Apoptosis in the rat brown adipose tissue after insulin treatment. *J Therm Biol* 1999;24:461–464.
- 31 Bachmeier M, Loffler G. Influence of growth factors on growth and differentiation of 3T3-L1 preadipocytes in serum-free conditions. *Eur J Cell Biol* 1995;68:323–329.
- 32 Hebert TL, Wu X, Yu G et al. Culture effects of epidermal growth factor (EGF) and basic fibroblast growth factor (bFGF) on cryopreserved human adipose-derived stromal/stem cell proliferation and adipogenesis. *J Tissue Eng Regen Med* 2009;3:553–561.
- 33 Kimura Y, Ozeki M, Inamoto T et al. Adipose tissue engineering based on human preadipocytes combined with gelatin microspheres containing basic fibroblast growth factor. *Biomaterials* 2003;24:2513–2521.
- 34 Xu JLK. Protein kinase B/AKT 1 plays a pivotal role in insulin-like growth factor-1 receptor signaling induced 3T3-L1 adipocyte differentiation. *J Biol Chem* 2004;279:35914–35922.
- 35 Baudry A, Yang ZZ, Hemmings BA. PKBalpha is required for adipose differentiation of mouse embryonic fibroblasts. *J Cell Sci* 2006;119:889–897.
- 36 Berwick DC HI, Heesom KJ, Moule SK et al. The identification of ATP-citrate lyase as a protein kinase B (Akt) substrate in primary adipocytes. *J Biol Chem* 2002;277:33895–33900.
- 37 Li XMB, Ge Q, Birnbaum MJ. Akt/PKB regulates hepatic metabolism by directly inhibiting PGC-1alpha transcription coactivator. *Nature* 2007;447:1012–1016.
- 38 Brown MS Goldstein J. A proteolytic pathway that controls the cholesterol content of membranes, cells, blood. *Proc Natl Acad Sci U S A* 1999;96:11041–11048.
- 39 Porstmann TGB, Chung YL, Delpuech O et al. PKB/Akt induces transcription of enzymes involved in cholesterol and fatty acid biosynthesis via activation of SREBP. *Oncogene* 2005;24:6465–6481.
- 40 Rommel C, Clarke BA, Zimmermann S et al. Differentiation stage-specific inhibition of the Raf-MEK-ERK pathway by Akt. *Science* 1999;286:1738–1741.
- 41 Font de Mora J, Porras A, Ahn N et al. Mitogen-activated protein kinase activation is not necessary for, but antagonizes, 3T3-L1 adipocytic differentiation. *Mol Cell Biol* 1997;17:6068–6075.
- 42 Bost F, Aouadi M, Caron L et al. The role of MAPKs in adipocyte differentiation and obesity. *Biochimie* 2005;87:51–56.
- 43 Beenken AMM. The FGF family: Biology, pathophysiology and therapy. *Nat Rev Drug Discov* 2009;8:235–253.
- 44 Citri A, Yarden Y. EGF-ERBB signalling: Towards the systems level. *Nat Rev Mol Cell Biol* 2006;7:505–516.
- 45 Harrington M, Pond-Tor S, Boney CM. Role of epidermal growth factor and ErbB2 receptors in 3T3-L1 adipogenesis. *Obesity (Silver Spring)* 2007;15:563–571.
- 46 Pagano E, Coso O, Calvo JC. Down-modulation of erbB2 activity is necessary but not enough in the differentiation of 3T3-L1 preadipocytes. *J Cell Biochem* 2008;104:274–285.
- 47 Pagano E, Calvo JC. ErbB2 and EGFR are downmodulated during the differentiation of 3T3-L1 preadipocytes. *J Cell Biochem* 2003;90:561–572.
- 48 Lenferink AE, Busse D, Flanagan WM et al. ErbB2/neu kinase modulates cellular p27(Kip1) and cyclin D1 through multiple signaling pathways. *Cancer Res* 2001;61:6583–6591.
- 49 Zhang X, Pickin KA, Bose R et al. Inhibition of the EGF receptor by binding of MIG6 to an activating kinase domain interface. *Nature* 2007;450:741–744.
- 50 Boucher J, Tseng YH, Kahn CR. Insulin and insulin-like growth factor-1 receptors act as ligand-specific amplitude modulators of a common pathway regulating gene transcription. *J Biol Chem* 2010;285:17235–17245.
- 51 Carver RS, Sliwkowski MX, Sitaric S et al. Insulin regulates heregulin binding and ErbB3 expression in rat hepatocytes. *J Biol Chem* 1996;271:13491–13496.
- 52 Lee H, Maihle NJ. Isolation and characterization of four alternate c-erbB3 transcripts expressed in ovarian carcinoma-derived cell lines and normal human tissues. *Oncogene* 1998;16:3243–3252.
- 53 Coleman SR. Long-term survival of fat transplants: Controlled demonstrations. *Aesthetic Plast Surg* 1995;19:421–425.
- 54 Ebrahimian TG, Pouzoulet F, Squiban Cet al. Cell therapy based on adipose tissue-derived stromal cells promotes physiological and pathological wound healing. *Arterioscler Thromb Vasc Biol* 2009;29:503–510.
- 55 Cervelli V, Gentile P, De Angelis B et al. Application of enhanced stromal vascular fraction and fat grafting mixed with PRP in post-traumatic lower extremity ulcers. *Stem Cell Res* 2011;6:103–111.
- 56 Garcia-Olmo D, Herreros D, Pascual I et al. Expanded adipose-derived stem cells for the treatment of complex perianal fistula: A phase II clinical trial. *Dis Colon Rectum* 2009;52:79–86.